JCI insight

RESEARCH ARTICLE

Atherogenesis and metabolic dysregulation in LDL receptor–knockout rats

Srinivas D. Sithu, Marina V. Malovichko, Krista A. Riggs, Nalinie S. Wickramasinghe, Millicent G. Winner, Abhinav Agarwal, Rihab E. Hamed-Berair, Anuradha Kalani, Daniel W. Riggs, Aruni Bhatnagar, and Sanjay Srivastava

Institute of Molecular Cardiology and Diabetes and Obesity Center, University of Louisville, Louisville, Kentucky, USA.

Mechanisms of atherogenesis have been studied extensively in genetically engineered mice with disturbed cholesterol metabolism such as those lacking either the LDL receptor (*Ldlr*) or apolipoprotein E (*apoe*). Few other animal models of atherosclerosis are available. WT rabbits or rats, even on high-fat or high-cholesterol diets, develop sparse atherosclerotic lesions. We examined the effects of *Ldlr* deletion on lipoprotein metabolism and atherosclerotic lesion formation in Sprague-Dawley rats. Deletion of *Ldlr* resulted in the loss of the LDLR protein and caused a significant increase in plasma total cholesterol and triglycerides. On normal chow, *Ldlr*-KO rats gained more weight and were more glucose intolerant than WT rats. Plasma proprotein convertase subtilisin kexin 9 (PCSK9) and leptin levels were higher and adiponectin levels were lower in KO than WT rats. On the Western diet, the KO rats displayed exaggerated obesity and age-dependent increases in glucose intolerance. No appreciable aortic lesions were observed in KO rats fed normal chow for 64 weeks or Western diet for 16 weeks; however, after 34–52 weeks of Western diet, the KO rats developed exuberant atherosclerotic lesions in the aortic arch and throughout the abdominal aorta. The *Ldlr*-KO rat may be a useful model for studying obesity, insulin resistance, and early-stage atherosclerosis.

Introduction

Atherosclerosis is the major underlying cause of peripheral artery disease, stroke, and ischemic heart disease. It is characterized by focal thickening and narrowing of the lumen of blood vessels due to the formation of lipid-laden plaques in the vessel wall. Although several factors contribute to the formation and the progression of atherosclerotic lesions, the central role of cholesterol in atherogenesis is well supported extensively by both experimental and epidemiological evidence (1–4). In humans, plasma cholesterol levels are strongly associated with cardiovascular disease (CVD) risk, and this risk is significantly mitigated by inhibitors of 3-hydroxy-3-methylglutaryl coenzyme A (HMG-CoA) reductase, such as statins (3, 4). Concordant data have been obtained from animal models. While most WT rodents maintain high HDl levels and do not develop atherosclerotic lesions, spontaneous mutations in the LDL receptor (LDLR) in Watanabe rabbits lead to hyperlipidemia and the development of diffuse atherosclerotic plaques (5). Similarly, genetically engineered mice lacking *Ldlr* or apolipoprotein E (*apoe*) are hyperlipidemic and develop exuberant atherosclerotic lesions throughout the arterial tree (6–9). Because they are amenable to genetic alterations and their arteries develop mature atherosclerotic plaques within a relatively short time, genetically engineered mice have become the models of choice for studying mechanisms of atherogenesis and for testing antiatherogenic interventions.

Although investigations using genetically altered mice have yielded important mechanistic insights into atherogenesis, these models have significant limitations. Atherosclerotic lesions in mice develop only under severe hypercholesterolemia, and the rate, site, and nature of these lesions are distinctly different from those of human atherosclerotic plaques (2). Moreover, the exclusive use of mouse models makes it difficult to rule out model- and species-dependent effects or to identify additional features of atherosclerosis that might be important in humans but not evident in mice. Hence, new animal models are needed to study the process of atherogenesis and to evaluate the role of hypercholesterol-

Conflict of interest: The authors have declared that no conflict of interest exists.

Submitted: January 19, 2016
Accepted: March 21, 2017
Published: May 4, 2017

Reference information:
JCI Insight. 2017;2(9):e86442. https://doi.org/10.1172/jci.insight.86442.

emia and other contributing factors to the formation of atherosclerotic lesions. In this manuscript, we describe a new rat model developed by the deletion of the *Ldlr*. This model could be useful for studying not only atherogenesis, but obesity and insulin resistance as well.

Results

Characterization of Ldlr-KO rats. Deletion of the *ldlr* gene using the zinc finger technology resulted in complete absence of LDLR protein in the liver (Figure 1A). There were no compensatory increases in the protein levels of the ATP-binding cassette, subfamily A, member 1 (ABCA1), and subfamily G1 (ABCG1) transporters. Moreover, deletion of *Ldlr* did not affect the mRNA levels of the other lipoprotein receptors; lipoprotein receptor–related proteins (LRP) such as LRP1B, LRP6, and LRP10; or the oxidized LDL related protein-1 (OLR1) in the liver; however, in comparison with WT rats, the hepatic levels of *vldlr* mRNA were moderately higher in the KO rats (Figure 1B), which might be an adaptive response to hypertriglyceridemia and the increase in VLDL in the KO rats. When placed on a normal chow (NC) diet, the plasma cholesterol levels in the KO rats were significantly higher in comparison with WT rats. As shown in Figure 1C, when these rats were 12 weeks of age, levels of the total plasma cholesterol in KO rats were 2.5-fold higher than WT rats. When monitored frequently, a progressive increase in total plasma cholesterol levels was noted in both WT and KO rats, and after 64 weeks, the plasma cholesterol levels in KO rats exceeded 400 mg/dl (Figure 1C). In addition to an increase in cholesterol, *Ldlr* deficiency also led to persistently elevated levels of plasma triglycerides (Figure 1D). Because *Ldlr* is the main route of degradation of proprotein convertase subtilisin kexin 9 (PCSK9) (10), we measured plasma level of this protein both in WT and *Ldlr* -KO rats. As shown in Figure 1E, loss of *Ldlr* was associated with a significant increase in circulating PCSK9 levels.

The dyslipidemic plasma profile was accompanied by lipid changes in the liver. In comparison with WT rats, the liver of KO rats had 2-fold higher levels of cholesterol and triglycerides (Table 1). However, despite dyslipidemia, there were no overt signs of hepatic or skeletal muscle injury in the KO rats, as their plasma levels of total protein, albumin, alanine aminotransferase (ALT), aspartate aminotransferase (AST), creatinine, and creatinine kinase (CK) were comparable with WT rats even at 64 weeks of age (Table 1). Likewise, no differences between plasminogen activator inhibitor-1 (PAI-1) and fibrinogen levels were observed between WT and KO rats. Separation of lipoproteins by size exclusion chromatography showed that, in comparison with WT rats, the VLDL and LDL + IDL fractions contained markedly higher levels of cholesterol, although the levels of cholesterol associated with the HDl fraction were lower in KO than WT rats (Figure 2, A and B). These data indicate that deletion of *Ldlr* results in a profound increase in the plasma levels of total cholesterol and triglycerides and a significant redistribution of cholesterol between different lipoprotein fractions, resulting in selective enrichment of cholesterol associated with VLDL. These changes are qualitatively similar to those that have been observed in *Ldlr*-KO mice (6), with the exception that — in contrast to *Ldlr*-KO mice, which show normal levels of triglycerides — the *Ldlr*-KO rats had 1.8-fold higher plasma triglyceride levels than WT rats.

Further characterization of lipoproteins in the KO rats indicated no appreciable change in the particle size of the different lipoprotein classes (Table 1). Because VLDL levels were elevated in KO rats, we examined changes in the plasma levels of apolipoprotein B (apoB), which is the major protein associated with VLDL. Deficiency of *Ldlr* did not affect the total apoB levels in the plasma (Figure 2C); however, silver staining of the protein separated on SDS-PAGE revealed that *Ldlr* deficiency was associated with an increase in the levels of apoB100 and in the apoB100/apoB 48 ratio (Figure 2D). In rodents, apoB100 is primarily cleared by the LDLR (11), whereas apoB48, which does not contain the LDLR binding region (12), is not recognized by the receptor. Hence, the relative increase in apoB100 vs. apoB48 in KO rats suggests a lack of *Ldlr*-mediated clearance of apoB100 containing VLDL particles. A similar increase in apoB100, relative to apoB48, has been observed in *Ldlr*-KO mice (11).

Because *Ldlr* deficiency was associated with an increase in triglycerides, we examined whether *Ldlr* deficiency affects hepatic triglyceride synthesis or degradation. To measure hepatic production of triglycerides, independent of their removal, we inhibited the clearance of plasma triglycerides using tyloxapol and measured the appearance of triglycerides in the plasma. We found that the rate of triglyceride secretion in KO rats was comparable with that obtained with WT rats (Supplemental Figure 1; supplemental material available online with this article; https://doi.org/10.1172/jci.insight.86442DS1), suggesting that the increase in plasma triglycerides is unlikely to be due to increased hepatic production of triglycerides. To examine changes in triglyceride degra-

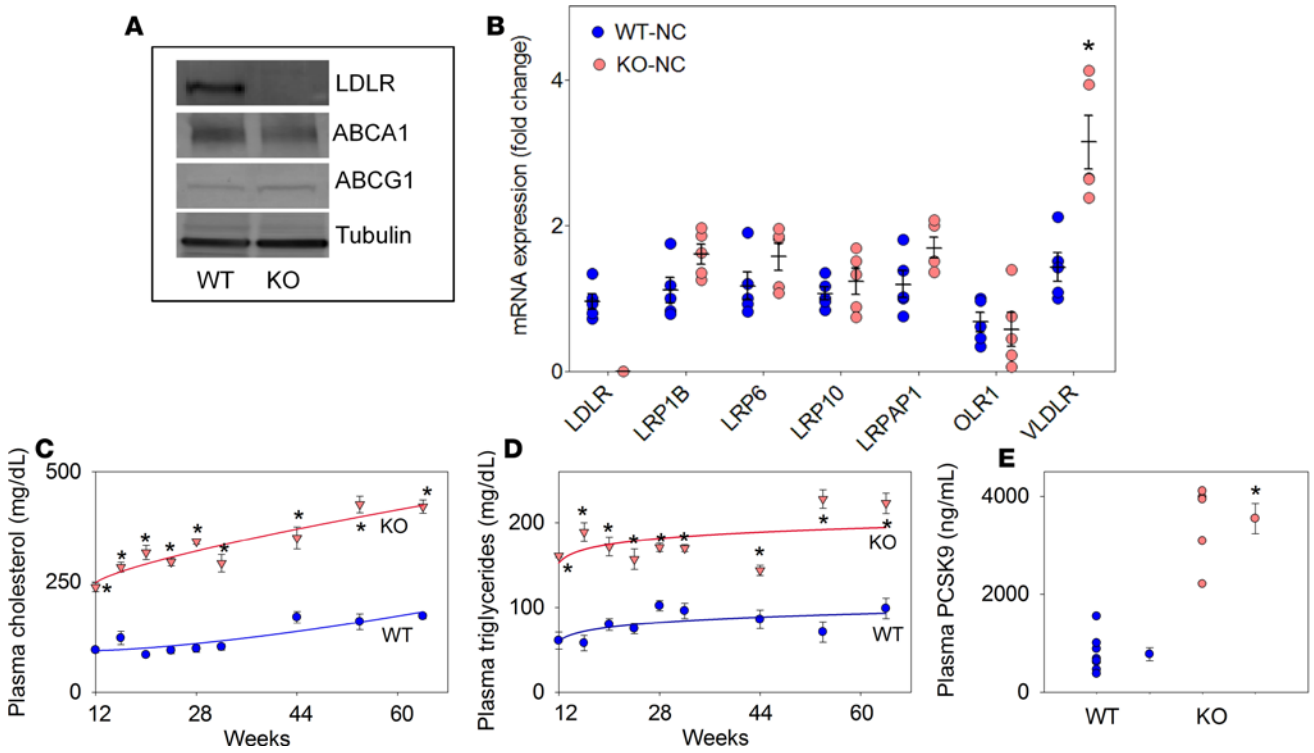

Figure 1. Dyslipidemia in *Ldlr*-KO rats. Rats were maintained on normal chow (NC) for 64 weeks, and blood and liver were collected following a 6h fast. (**A**) Representative Western blots (n = 3–4/group) of liver homogenates of *Ldlr*-KO and WT rats probed with anti–LDL receptor; anti-ATP–binding cassette, subfamily A, member 1 (ABCA1); and anti-ATP–binding cassette, subfamily G1 (ABCG1) antibodies. (**B**) Quantitative PCR analyses for the mRNA expression of lipoprotein receptors in the liver of *Ldlr*-KO and WT rats (n = 5/group). (**C** and **D**) The time course of plasma cholesterol and triglyceride levels respectively of *Ldlr*-KO (n = 5–9) and WT (n = 5–9) rats. (**E**) The plasma proprotein convertase subtilisin kexin 9 (PCSK9) levels in 62-week-old rats (n = 6–8/group). Unpaired 2-tailed Student's t test was used for the analyses of data in panels **B** and **E**, and 2-way ANOVA was used for the analyses of data in panels **C** and **D**. Values are mean ± SEM. *P < 0.05 vs. WT rats.

dation, we examined the apoA-V–lipoprotein lipase (LPL) axis. Previous studies have shown that apoA-V, associated with HDl and VLDL particles, promotes hydrolysis of triglycerides by activating LPL (13). As shown in Figure 2E, the levels of apoA-V were 18% lower in KO than WT rats. This was accompanied by a 75% decrease in LPL activity (Figure 2F). Taken together, these observations suggest that hypertriglyceridemia in KO rats may be in part related to decreased lipolysis and catabolism of triglycerides via LPL.

During our studies, we noticed that the body weight of the *Ldlr*-KO rats was significantly higher than WT rats. At 12 weeks of age, the KO rats fed NC were 1.5-fold heavier than WT rats. Even after 64 weeks, the body weight of KO rats was significantly higher than age-matched WT rats (Figure 3, A and B). To examine the obesogenic phenotype of KO rats in greater detail, we measured their blood glucose, insulin, and adipokine levels and determined their glucose tolerance. We found that the fasting blood glucose levels in KO rats were similar to those of WT rats until they were 42 weeks of age (data not shown), and plasma insulin levels were > 2 fold higher than WT rats. As a result, the homeostatic model assessment-insulin resistance (HOMA-IR) scores obtained from KO rats were consistently higher than WT rats (Figure 3, C–F). When subjected to glucose tolerance tests (GTTs), the KO rats showed lower rates of glucose clearance than WT rats, but the 2 strains had comparable insulin tolerance (data not shown). The glucose intolerance of KO rats was apparent when the rats were 18 weeks old, and it worsened progressively with age (Figure 3, C–F). Moreover, in comparison with WT rats, the plasma of KO rats had 3-fold higher levels of leptin and 40% lower adiponectin levels (Table 1). This was accompanied by 1.5-fold higher plasma levels of nonessential fatty acids (NEFA; Table 1). Taken together, these results suggest that the loss of *Ldlr* in rats promotes progressive weight gain and glucose intolerance.

Effect of Western diet. To examine whether increased fat intake would exacerbate dyslipidemia, obesity, and glucose intolerance in KO rats, we placed WT and KO rats on a Western diet (WD). We found that consumption of WD led to a progressive increase in the plasma cholesterol levels in KO rats, whereas the plasma cholesterol levels of WT rats placed on a similar diet were only marginally affected (Figure 4A). After 52 weeks on

Table 1. Parameters measured in the plasma and liver of Ldlr-KO rats

Parameters	WT-NC	KO-NC	WT-WD	KO-WD
Plasma				
Albumin (g/dl)	3.58 ± 0.05	3.52 ± 0.09	4.11 ± 0.14	4.89 ± 0.30
Total protein (g/dl)	6.52 ± 0.20	6.82 ± 0.25	8.97 ± 0.39	24.32 ± 4.44^{A,B}
ALT (U/l)	54 ± 6	39 ± 1	28 ± 4^{C}	209 ± 71^{A,B}
AST (U/l)	159 ± 16	112 ± 18	140 ± 20	249 ± 74
CK (U/l)	670 ± 93	354 ± 90	996 ± 183	527 ± 96
Creatinine (mg/dl)	0.59 ± 0.04	0.53 ± 0.04	0.59 ± 0.03	2.45 ± 0.79^{A,B}
BUN (mg/dl)	21 ± 2	14 ± 1	16 ± 1	13 ± 2
PAI-1 (ng/ml)	9.31 ± 0.79	10.36 ± 0.49	12.86 ± 1.6	14.15 ± 1.27
Fibrinogen (mg/ml)	3.14 ± 0.13	2.87 ± 0.167	3.08 ± 0.09	3.21 ± .321
Leptin (ng/ml)	9.83 ± 0.68	28.18 ± 4.14^{C}	34.72 ± 2.72^{C}	65.59 ± 7.52^{A,B}
Adiponectin (μg/ml)	82.96 ± 4.73	48.4 ± 5.6^{C}	83.97 ± 5.17	58.27 ± 7.02^{B}
NEFA (mmol/L)	0.52 ± 0.04	0.78 ± 0.12^{C}	1.23 ± .15^{C}	2.95 ± .63^{A,B}
Lipoproteins				
Chylomicrons+VLDL cholesterol (mg/dl)	10 ± 1	178 ± 26^{C}	29 ± 6^{C}	1495 ± 48^{A,B}
IDL+LDL cholesterol (mg/dl)	94 ± 16	168 ± 8^{C}	139 ± 12^{C}	943 ± 85^{A,B}
HDl (mg/dl)	69 ± 11	73 ± 6	54 ± 5	81 ± 11^{A,B}
VLDL particle size (nm)	38.0 ± 1.5	35.8 ± 0.1	95.0 ± 7.0^{C}	68 ± 4^{A,B}
LDL particle size (nm)	22.7 ± 0.1	22.9 ± 0.1	22.6 ± 0.1	22.9 ± 0.1
HDl particle size (nm)	11.6 ± 0.3	13 ± 0.1	11.7 ± 0.4	8.9 ± 0.1^{A}
Liver				
Cholesterol (mg/g tissue)	5.39 ± 0.14	10.38 ± 2.17^{C}	21.11 ± 3.4^{C}	35.43 ± 3.17^{A,B}
Triglycerides (mg/g tissue)	13.12 ± 1.35	25.76 ± 5.72^{C}	7.76 ± 0.72^{C}	18.77 ± 1.74^{B}

Values are mean ± SEM of rats maintained on normal chow (NC) for 64 weeks or 12-week-old rats maintained on Western diet (WD) for 52 weeks. $^{A}P < 0.05$ vs. *Ldlr*-KO–NC, $^{B}P < 0.05$ vs. WT-WD, $^{C}P < 0.05$ vs. WT-NC. Alanine aminotransferase, ALT; aspartate aminotransferase, AST; creatinine kinase, CK; blood urea nitrogen, BUN; nonessential fatty acids, NEFA; PAI-1, plasminogen activator inhibitor-1.

WD, the plasma levels of cholesterol in KO rats were 10-fold higher than the NC-fed rats or WT rats fed a WD. A similar progressive increase in plasma triglycerides was observed in KO rats fed WD, such that after 52 weeks, the plasma triglyceride levels were 4-fold higher in the KO than WT rats (Figure 4B). The KO rats also had 8-fold higher levels of plasma PCSK9 levels than WT rats (Figure 4C). A similar increase in circulating PCSK9 levels has been reported in *Ldlr*-KO mice maintained on WD (14). FPLC separation of plasma lipoproteins showed that, similar to normal chow-fed KO rats, WD-fed KO rats displayed significantly higher levels of VLDL and LDL + IDL cholesterol (Figure 4D). Consumption of WD also upregulated the levels of ABCA1 in the liver of KO rats, although the levels of ABCG1 remained unchanged (Figure 4E). Plasma LPL protein levels in WD-fed KO rats were comparable with WD-fed WT rats (data not shown). However, WD significantly decreased the plasma apoA-V levels (Figure 4F) and LPL activity in KO rats (Figure 4G). Hepatic cholesterol and triglycerides were also significantly higher in WD-fed KO rats (Table 1). Measurements of hepatic triglyceride production after inhibition of triglyceride clearance by tyloxapol showed that, as with rats on NC, the WT or KO rats fed WD for 1 week did not show an increase in the appearance of triglycerides in the plasma (Supplemental Figure 1). Indeed, the rate of triglyceride production in KO rats was lower than in WT rats, which may be a compensatory mechanism to limit excessive triglycerides in the plasma. The KO rats also showed significant increases in total plasma protein, creatinine, and ALT levels, while minimal changes were observed in WT rats (Table 1). However, blood urea nitrogen (BUN) levels in WD-fed KO rats were comparable with corresponding WT rats.

In addition to exacerbating dyslipidemia, consumption of WD also aggravated weight gain and glucose intolerance. As shown in Figure 5, A and B, we found that rats placed on WD showed a progressive increase in weight gain, which was much more pronounced in KO than WT rats. After 52 week on WD, the weight of the KO rats was 1.5-fold higher than the KO rats fed NC and exceeded 1 kg (Figure 5A). Feeding WD increased the plasma levels of leptin and NEFA in WT rats without affecting the plasma levels of adiponectin. However, WD-induced changes in leptin and NEFA were much more severe in KO rats than

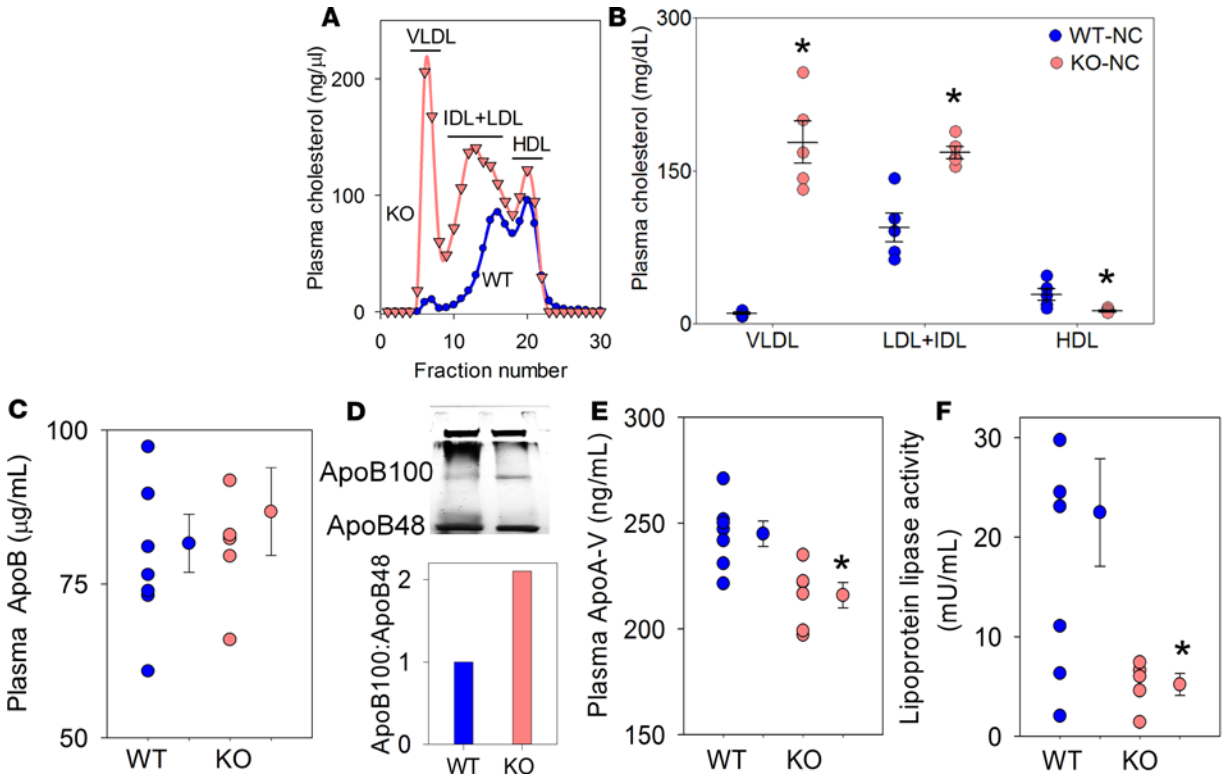

Figure 2. Plasma lipoproteins in *Ldlr*-KO rats. Lipoprotein profiles of WT and *Ldlr*-KO rats maintained on normal chow (NC) for 64 weeks. (**A**) Representative chromatogram of the separation of lipoproteins on fast protein liquid chromatography (FPLC) on a Superose 6 column equilibrated with PBS. Plasma was applied to the column, and samples were eluted isocratically with PBS. Cholesterol recovered in FPLC eluate (0.5 ml fractions) was measured as described in Methods. Data show levels of cholesterol in 125 ml WT and 50 ml KO plasma. (**B**) Abundance of total lipoproteins in the plasma (n = 5/group). (**C** and **D**) Levels of total apolipoprotein B (apoB) in the plasma (n = 6–8/group) and relative distribution of apoB100 and apoB48 in the VLDL obtained from delipidated plasma (pooled from 5 rats/group), separated on 3% SDS-PAGE and silver stained. (**E** and **F**) Plasma apolipoprotein A-V (apoA-V) levels and lipoprotein lipase activity, respectively (n = 5–8/group). Unpaired 2-tailed Student's t test was used for data analyses. Values are mean ± SEM. *P < 0.05 vs. WT rats.

WT rats, with a corresponding decrease in adiponectin levels (Table 1). Feeding WD led to a progressive increase in glucose intolerance in KO, which was more pronounced in KO than WT rats (Figure 5, C–E). At all ages tested, the HOMA-IR scores (Figure 5, C–E, insets) and the AUC from GTT (Figure 5F) were higher in KO than WT rats, and the difference between WT and KO rats was much greater when the rats were of 52 weeks of age than when they were 12 weeks old. The WD had no effect on plasminogen activator inhibitor-1 (PAI-1) and fibrinogen levels in either WT or KO rats (Table 1). Taken together, these data suggest that deletion of *Ldlr* exaggerates the metabolic effects of WD.

Atherosclerotic lesion formation. When maintained on NC or WD, the KO rats did not show appreciable atherosclerotic lesion formation either in the aortic valve or the aorta for 16–18 weeks (Figure 6), but after 34 weeks of WD, sporadic atherosclerotic lesions were observed in the aortic root (Figure 6A) and the abdominal aorta (Figure 6B). However, after 42 weeks, robust atherosclerotic plaques were seen in the aortic arch, the thoracic aorta, and the abdominal aorta (Figure 6B). Mean lesion area in the aorta of KO rats maintained on WD for 52 weeks was 33% ± 5%. Moreover, in 4 of 5 KO rats, atherosclerotic lesions were detected in the proximal end of the coronary arteries (Figure 6C). Coronary lesions were detected up to 120 μm from the site of origin of the coronary arteries, but such lesions were rarely seen in the distal artery. No lesions were detected anywhere in the aortic tree of WT rats either on NC or WD (Figure 6). These observations suggest that atherosclerotic lesions develop in KO rats only after prolonged WD feeding.

To examine whether cholesterol lowering facilitates plaque regression, we placed 12-week-old *Ldlr*-KO rats on WD for 44 weeks for the lesions to develop. The rats were then placed on NC for 8 weeks. We found that withdrawal of WD for 8 weeks decreased plasma cholesterol by 55% (P < 0.05), but it did not affect the size of the aortic lesions (data not shown). Further studies with prolonged cholesterol withdrawal or lipid lowering therapies are required to examine if the lesions in KO rats can be regressed.

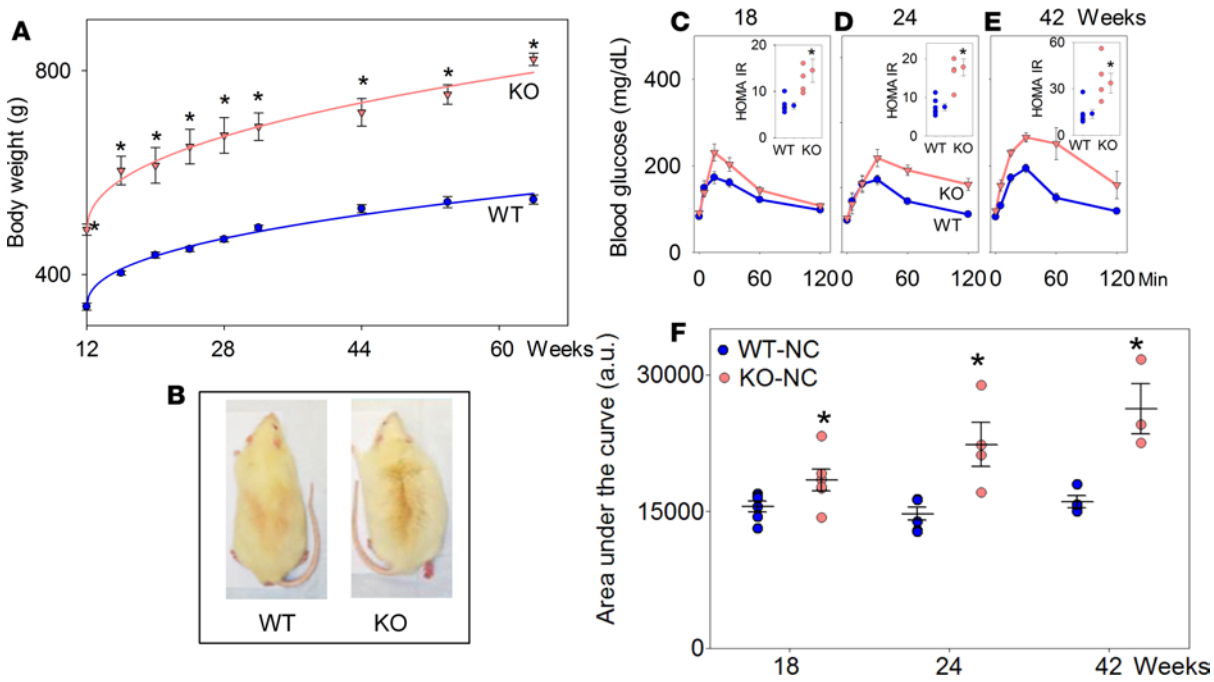

Figure 3. Metabolic changes in *Ldlr*-KO rats. (**A**) WT and *Ldlr*-KO rats were maintained on normal chow (NC) for 64 weeks, and body weights were measured at indicated time points (n = 5–12/group). (**B**) The representative picture of rats maintained on NC for 64 weeks. (**C**–**F**) Glucose (1 g/kg; i.p.) tolerance test (GTT) in KO rats maintained on NC for 18 (**C**), 24 (**D**) and 42 (**E**) weeks. Insets show the corresponding homeostatic model assessment-insulin resistance (HOMA-IR) levels (n = 5–6). (**F**) The AUC for GTT (n = 3–6/group). Two-way ANOVA was used for the analyses of data in **A** and **F**, and unpaired 2-tailed Student's t test was used for the analyses of data in insets of panels **C**–**E**. Values are mean ± SEM. *$P < 0.05$ vs. WT rats.

Because high levels of cholesterol could stimulate inflammatory responses, we examined inflammation both in the lesions and in circulation. Staining of the lesions of the abdominal aorta with anti-CD68 antibody showed the accumulation of $CD68^+$ macrophages in the intima (Figure 6D). Intimal lesions also showed appreciable staining for TNFα, monocyte chemoattractant protein-1 (MCP-1), and cytokine IL-6 (Figure 6D). Quantitation of cytokines and chemokines in the plasma showed that cytokines such as macrophage inflammatory protein-2 (MIP-2), TNFα, IFNγ, IL-1α, and IL-1β were abundant in KO rats with lesions (52 weeks of WD) but were undetectable in the plasma of corresponding KO rats maintained on NC (Table 2). Plasma levels of inflammatory cytokines and chemokines including IFNγ; RANTES (CCL5) — which stimulates the chemotaxis of T cells, eosinophils, and basophils — along with neutrophil chemoattractant-lipopolysaccharide–inducible CXC chemokine (LIX; CCR5) and KC (IL-8) were also significantly elevated in the plasma of KO-WD than KO-NC rats. Interestingly, levels of antiinflammatory cytokines IL-10 and IL-4 were also higher in WD-fed KO rats than in NC-fed KO rats. However, plasma levels of IL-6 and MCP-1 — as well as several other monocyte/macrophages chemoattractant proteins, such as MIP1α, fractalkine, and IP-10 — were not affected by the diet. Together, these data suggested that the formation of atherosclerotic lesions in KO rats was accompanied by pervasive systemic inflammation, as well as lesion-specific inflammation. However, the abundance of specific chemokines and cytokines (e.g., IL-6 and MCP-1) in the lesions does not correlate with their plasma levels. These inflammatory changes are similar to those that have been described in mouse atherosclerotic lesions.

Discussion

The LDLR belongs to a family of cell surface receptors that bind and internalize extracellular ligands (15, 16). Binding of the receptor to a single copy of apoB100 present in LDL leads to endocytosis of the complex and removal of LDL from circulation. In humans, this process mediates approximately two-thirds of LDL clearance, and loss-of-function mutations in the LDLR are associated with familial hypercholesterolemia (FH), a genetic disorder characterized by severe hypercholesterolemia, accelerated CVD, and early death (15, 16). In contrast, mice lacking *Ldlr* show a moderate increase in LDL levels but do not develop atherosclerotic lesions unless placed on a high-cholesterol diet (6). Atherosclerotic lesions in mice develop only with extreme hyper-

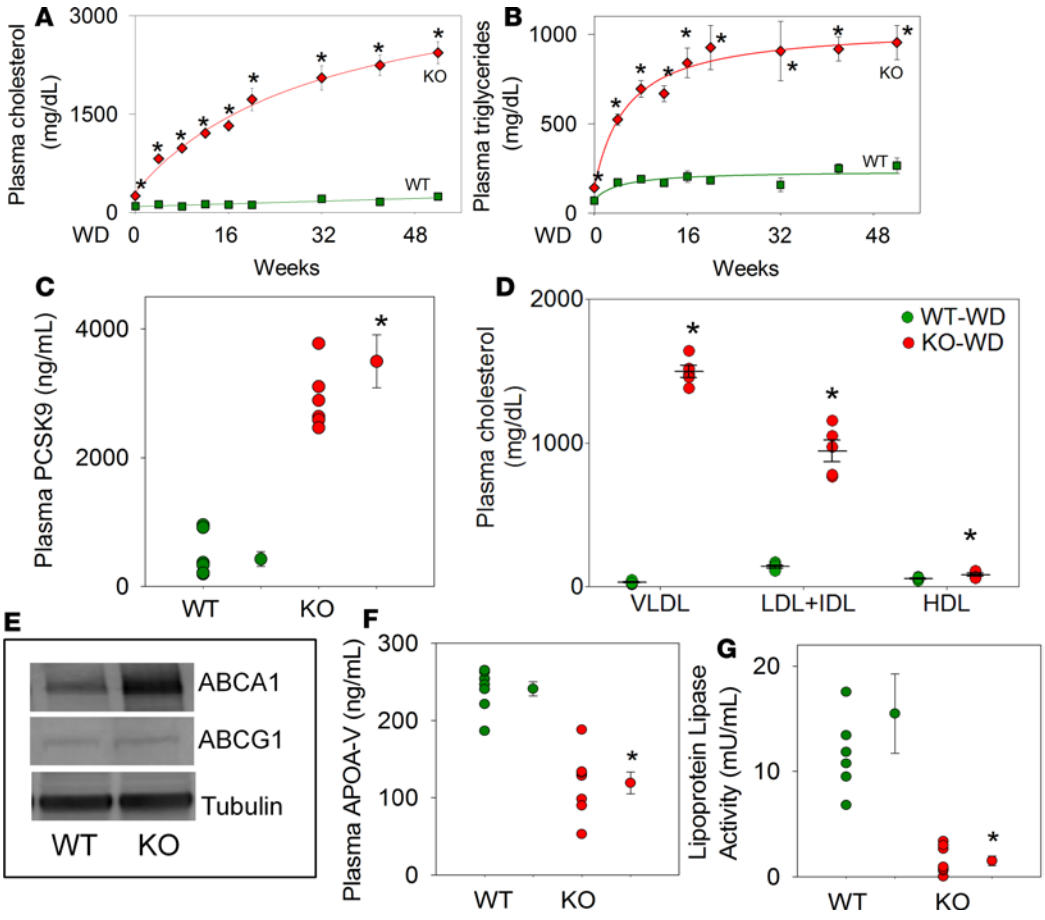

Figure 4. Effect of Western diet on dyslipidemia in *Ldlr*-KO rats. Twelve-week-old WT and *Ldlr*-KO rats were maintained on Western diet (WD) for 52 weeks. Plasma cholesterol (**A**; n = 8–10/group) and triglycerides (**B**; n = 8–10/group) were measured at indicated time point following 6h of starvation. (**C**) Plasma proprotein convertase subtilisin kexin 9 (PCSK9) levels were measured by ELISA after 52 weeks of WD (n = 8/group). (**D**) Abundance of total lipoproteins in the plasma (n = 5 per group). (**E**) Representative Western blots (n = 3/group) of ATP-binding cassette, sub-family A, member 1 (ABCA1) and ATP-binding cassette, sub-family G1 (ABCG1) proteins in the liver of rats. (**F** and **G**) Plasma apolipoprotein A-V (apoA-V) levels and lipoprotein lipase activity (n = 8/group). Two-way ANOVA was used for the analyses of data in **A** and **B** and unpaired 2-tailed Student's t test was used for the analyses of data in insets of panels **C**, **D**, **F**, and **G**. Values are mean ± SEM. *$P < 0.05$ vs. WT rats.

cholesterolemia, and the rate, site, and the nature of lesion formation are different from humans (2). Hence, we examined the effects on *Ldlr* deletion on rats, which differ from mice in their inflammatory responses and cholesterol metabolism. Our results show that, in rats, *Ldlr* deletion was associated with increased VLDL and LDL + IDL cholesterol and a suppression of HDl levels. However, as in mice (6), *Ldlr* deletion in rats did not lead to the formation of atherosclerotic lesions on NC, although significant formation of atherosclerotic lesions was observed when these rats were placed on WD. Importantly, in contrast to mice, *Ldlr* deletion in rats was associated with progressive obesity and glucose intolerance, conditions that were further exacerbated by WD. This unique phenotype of the *Ldlr*-KO rat could reveal novel relationships between dysregulated cholesterol metabolism and its functional consequences. Therefore, the *Ldlr*-KO rat could be a new model that is useful for studying cholesterol metabolism as well as the mechanisms underlying early atherogenesis, particularly in the context of diabetes and obesity. Moreover, the model could be useful for studying the effects of toxicants, tobacco products, drugs, and environmental pollutants on diet-independent effects on dyslipidemia and insulin resistance, and diet-dependent formation of atherosclerotic lesions.

The relationship between dyslipidemia and atherosclerosis has been studied extensively in several animal models including mice, (2, 6, 7) rabbits (17), rats (18), and pigs (19–21); however, the effects of *Ldlr* deletion have not been assessed in rats, although the effects of a mutation in the LDLR binding domain have been evaluated (22). Results from these animal models show that, even though *Ldlr* deficiency or dysfunction is universally associated with an increase in LDL cholesterol and a suppression of HDl levels, changes in systemic metabolism and plasma lipoproteins, and the formation of atherosclerotic lesions are variably affected. For instance, in comparison with humans, the *Ldlr*-KO mice show milder hypercholesterolemia, which may be related to differences in lipoprotein composition between the 2 species. Unlike the human liver, the mouse liver synthesizes 2 forms of apoB — apoB100 and apoB48 — both of which are incorporated in VLDL (23). Because apoB100 is the principle LDLR binding domain, deletion of the receptor prevents the uptake of apoB100 containing lipoproteins, but not apoB48, which could be cleared by LDLR-independent mechanisms. As a result, mice lacking *Ldlr* develop less severe hypercholesterolemia than homozygous FH patients

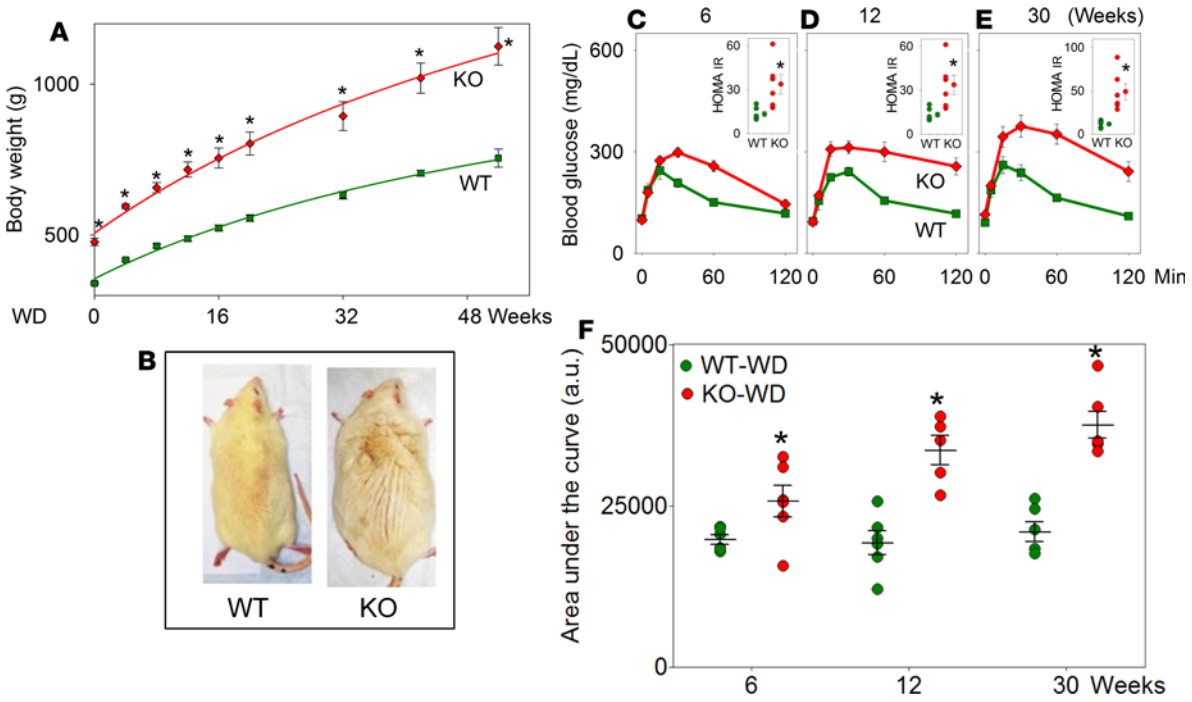

Figure 5. Effect of Western diet on metabolic parameters in *Ldlr*-KO rats. Twelve-week-old WT and *Ldlr*-KO rats (n = 8–12/group) were maintained on WD for 0–52 weeks. (**A**) Time course of the effect of WD on body weight. (**B**) Representative picture of rats maintained on WD for 52 weeks. (**C**–**F**) Glucose (1 g/kg; i.p.) tolerance test (GTT) of rats maintained on WD for 6 (**C**), 12 (**D**), and 30 (**E**) weeks. Insets show the corresponding homeostatic model assessment-insulin resistance (HOMA-IR) levels (n = 5–6/group). (**F**) The AUC for GTT (n = 5–6/group). Two-way ANOVA was used for the analyses of data in panels **A** and **F**, and unpaired 2-tailed Student's t test was used for the analyses of data in insets of panels **C**–**E**. Values are mean ± SEM. *$P < 0.05$ vs. WT rats.

(6). Like the mouse liver, the rat liver also synthesizes both apoB100 and apoB48, but in rats, apoB100 undergoes further editing to form apoB95 (24). The consequences of these differences in apoB isoforms remain poorly understood; however, hypertriglyceridemia seen in *Ldlr*-KO rats, but not *Ldlr*-KO mice, and a relatively mild increase in LDL + IDL cholesterol in *Ldlr*-KO rats (1.5-2.0-fold; this study) vs. *Ldlr*-KO mice (8-fold) (6) suggest that the effects of *Ldlr*-deletion on the liver cholesterol metabolism and the resultant adaptive changes in cholesterol synthesis and transport are likely to be different between mice than rats.

In addition to removing LDL from circulation, the LDLR also regulates the secretion of apoB proteins in both mice and humans. Patients with FH overproduce IDL and LDL (25) and experiments with *Ldlr*-KO mice have shown that LDLR mediates the reuptake of newly synthesized apoB containing lipoprotein particles and thereby alters the proportion of apoB that escapes co- and posttranslational presecretory degradation of apoB (26). The *Ldlr* mediates the presecrectory degradation of both apoB100- and apoB48-containing proteins that interact with the receptor via apoB100 and apoE, respectively. Indeed, transgenic mice overexpressing apoE have hypertriglyceridemia due to a combination of enhanced VLDL secretion and decreased LPL-mediated lipolysis of VLDL (27). Therefore, the differences in dyslipidemia between *Ldlr*-KO mice and rats may relate to differences in ratio of apoB100/apoB48 synthesized in the rat vs. the mouse liver and the extent to which VLDL is degraded by the LDLR-mediated mechanism in the rat. While direct comparative measurements are lacking, our data showing that the apoB100/apoB48 ratio is 2 in *Ldlr*-KO rats but 4 in *Ldlr*-KO mice (6) indicate that more apoB48 is generated in the rat than the mouse liver — or that more apoB48 is degraded via LDLR in rats than in mice — leading to more pronounced hypertriglyceridemia in *Ldlr*-KO rats than *Ldlr*-KO mice. That the LDLR regulates triglyceride metabolism, and secretion is further supported by the observation that targeted disruption of LDLR in Yucatan mini pigs leads to a 50-fold increase in VLDL after 26 weeks of age (20). Similarly, downregulation of LDLR in mice by transgenic expression of PCSK9, which degrades LDLR protein, results in an increase in fasting serum triglyceride and VLDL levels, even in chow-fed animals (28). Mice overexpressing human D347Y-PCSK9, the gain of function of missense mutation associated with severe familial hypercholesterolemia, also secrete more triglycerides than WT mice (29). Hence,

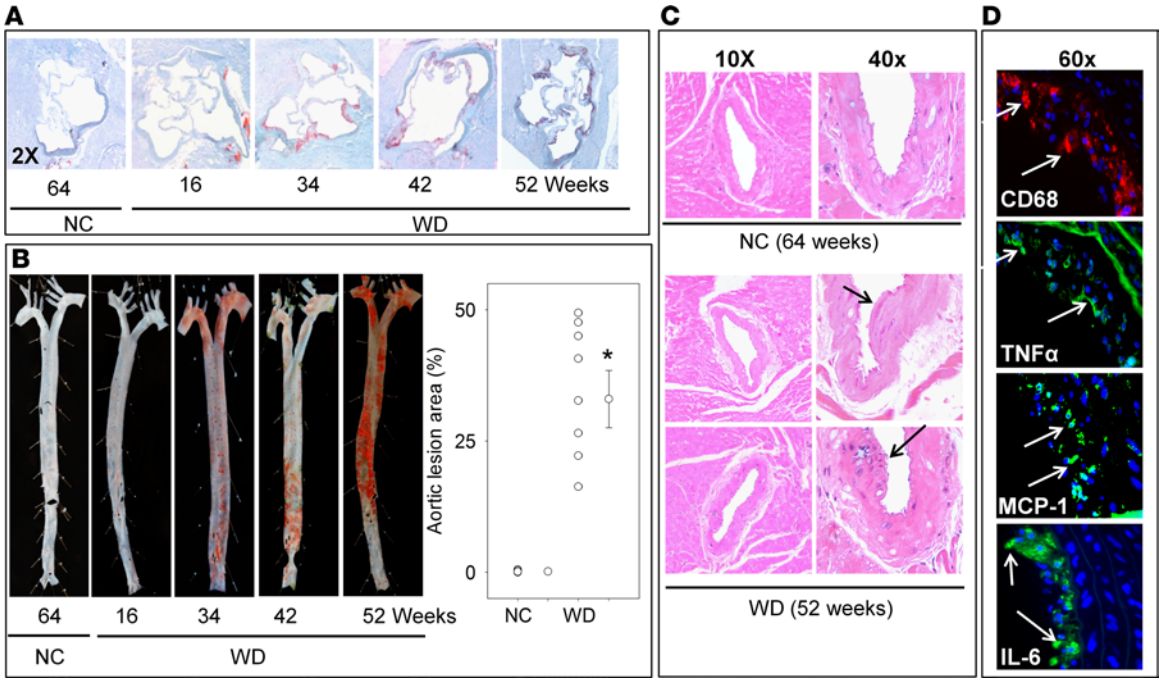

Figure 6. Atherosclerotic lesion formation in *Ldlr*-KO rats. Twelve-week-old male WT or *Ldlr*-KO rats were either maintained on normal chow (NC) or Western diet (WD) for up to 52 weeks. Lipids in the aortic valve (**A**) were stained with Oil Red O and in the aorta with Sudan IV (**B**). Unpaired 2-tailed Student's *t* test was used for the statistical analyses of aortic lesions. Values are mean ± SEM. **P* < 0.05 vs. WT rats. (**C**) Photomicrographs of lesions in the H&E-stained sections of coronary artery of *Ldlr*-KO rats maintained on NC for 64 weeks (*n* = 4) or WD for 52 weeks (*n* = 6). (**D**) Photomicrographs of the sections (*n* = 3/group) of the distal aorta stained with anti-CD68 (red), -TNFα (green), –monocyte chemoattractant protein-1 (MCP-1) (green), and –IL-6 (green) antibodies. Nuclei are stained with DAPI (blue). Arrows indicate lesions.

the increase in triglycerides seen in *Ldlr*-KO rats may be related in part to the increase in PCSK9 seen in these animals, leading to increased apoB secretion (14). Further experiments using PCSK9 inhibitors are required to identify the role of PCSK9 in regulating apoB secretion in *Ldlr*-KO rats.

An additional factor contributing to hypertriglyceridemia in *Ldlr*-KO rats may be related to changes in the LPL–apoA-V axis. Since LPL transforms chylomicrons to remnants and facilitates the conversion of VLDL to LDL, a decrease in LPL activity could increase VLDL. In humans, elevated plasma LPL activity is associated with decreased triglycerides and an increase in HDl cholesterol, and heterozygotes for LPL deficiency have augmented levels of circulating triglycerides and decreased HDl levels (30). While reasons for LPL deficiency secondary to *Ldlr* deletion remain unclear, the decrease in the activity of the enzyme might be related to the observed decrease in apoA-V in *Ldlr*-KO rats. In the plasma, apoA-V is found predominantly bound to VLDL and HDl, and it activates proteoglycan-bound LPL to enhance triglyceride hydrolysis (31–33). In humans, several polymorphic forms of the apoA-V gene have been reported to be associated with hypertriglyceridemia and impaired LPL activity (34, 35). Carriers of rare nonsynonymous mutations of apoA-V in humans have higher plasma triglyceride levels, as well (36). Studies in experimental animals show that deficiency of apoA-V in WT mice increases the plasma levels of triglycerides by 4-fold, and overexpression of human apoA-V transgene decreases plasma triglycerides by 30% (37). Moreover, overexpression of human apoA-V in *apoe*-KO or *apoe*2-knockin mice significantly decreases plasma triglyceride levels (37). Hence, the observed decrease in apoA-V and LPL activity could in part account for hypertriglyceridemia in *Ldlr*-KO rats. In addition, the increase in plasma triglyceride levels could also be due to suppression of adiponectin levels even in rats maintained on NC. In dyslipidemic (38) and diabetic subjects (39) plasma adiponectin levels are inversely related with triglycerides, and adiponectin has been suggested to decrease plasma triglycerides by increasing VLDL catabolism in the skeletal muscle without affecting the rate of hepatic apoB secretion (40). Thus, the decrease in adiponectin levels in *Ldlr*-KO rats could, in part, account for the observed hypertriglyceridemia in these rats. Because adiponectin secretion by adipocytes is decreased upon lipid accumulation, an initial increase in circulating triglycerides in *Ldlr*-KO rats could set up a vicious cycle in which lipid accumulation in adipocytes suppresses adiponectin secretion, which in turn could further exacerbate hypertriglyceridemia by diminishing VLDL catabolism.

Table 2. Plasma cytokine levels in Ldlr-KO rats

Cytokine (pg/ml)	KO-NC	KO-WD
MIP-2 (CXCL2)	ND	16 ± 2
MIP-1α	6.7 ± 0.8	12.0 ± 1.7
Fractalkine (CX3CL1)	31 ± 9	21 ± 6
IP-10 (CXCL10)	113 ± 20	150 ± 20
MCP-1	157 ± 16	280 ± 45
RANTES (CCL5)	77 ± 14	274 ± 72[A]
LIX (CXCL5)	331 ± 60	1,476 ± 239[A]
GRO/KC	7.1 ± 0.9	24 ± 5[A]
Eotaxin (CCL11)	ND	5.3 ± 0.6[A]
TNFα	ND	2.5 ± 1.0[A]
IFNγ	ND	23 ± 12[A]
IL-1α	ND	16 ± 4[A]
IL-1β	ND	290 ± 89[A]
IL-2	27 ± 14	39 ± 9
IL-4	11 ± 2	25 ± 3[A]
IL-5	ND	ND
IL-6	140 ± 56	307 ± 25[A]
IL-10	ND	241 ± 106[A]
IL-12p70	ND	24 ± 6[A]
IL-13	ND	11.5 ± 2.0[A]
IL-17A	ND	ND
IL-18	57 ± 28	71 ± 6
EGF	0.4 ± 0.1	0.9 ± 0.1[A]
VEGF	21 ± 10	27 ± 5
G-CSF	ND	ND

Values are mean ± SEM of KO rats maintained on normal chow (NC) for 64 weeks or 12 weeks old KO rats maintained on Western diet (WD) for 52 weeks. [A]$P < 0.05$ vs. KO-NC. ND, not detectable.

The increase in VLDL levels and triglycerides in *Ldlr*-KO rats was associated with increased adiposity and progressive glucose intolerance (41). This increase in obesity and glucose intolerance has not been reported in other models of LDLR deficiency or dysfunction. The *Ldlr*-KO mice on NC do not gain more weight than their WT controls, and they maintain normal insulin and leptin levels and glucose intolerance (42, 43). Similarly, no increase in weight gain or hyperglycemia has been reported in pigs expressing PCSK9 gain-of-function mutations (21) or with *Ldlr* deficiency (20). Moreover, like the *Ldlr*-KO mice, the *apoe*-KO mice are also resistant to metabolic changes and do not show changes in triglyceride and glucose metabolism, even on a WD (44). Thus, increased obesity and insulin resistance in *Ldlr*-KO rats is surprising, particularly because these changes are observed in the presence of elevated plasma PCSK9 levels. It has been previously suggested that because, in addition to LDLR, PCSK9 also targets VLDLR and CD36 (45), lack of PCSK9 can increase the expression of VLDLR or CD36 to facilitate triglyceride hydrolysis and free fatty acid uptake in visceral adipocytes (46). Indeed, mice with PCSK9 deficiency exhibit impaired glucose tolerance and insulin resistance (47). In contrast, the *Ldlr*-KO rats developed insulin resistance, glucose intolerance, and obesity even with an 8- to 10-fold higher plasma PCSK9 levels, indicating that increased PCSK9-mediated degradation of VLDLR in these rats, if any, is not sufficient to prevent lipid accumulation in the adipocytes or the liver.

When placed on a WD, the *Ldlr*-KO rats showed signs of mild hepatic injury, as reflected by an increase in ALT levels and renal dysfunction, as evidenced by an increase in plasma creatinine levels. However, WD did not increase BUN levels in the KO rats. Usually with frank renal injury, both the levels of BUN and creatinine increase with a corresponding increase in the BUN/creatinine ratio (48, 49), but feeding WD led to a decrease (from 23 to 5) rather than an increase in this ratio, which might be indicative of incipient rather than frank renal dysfunction. Feeding the WD also increased total plasma protein, although the levels of albumin were not affected. Given that plasma proteins comprise mainly albumin and globulin, we speculate that the WD-induced increase in plasma proteins may be reflective of systemic inflammation. Indeed, we found that KO rats on WD had higher levels of several inflammatory, as well as antiinflammatory cytokines (Table 2). Similar extensive increases in plasma cytokines have been observed in other animal models of dyslipidemia (50–52) and are thought to be secondary to the activation of immune responses due to persistently high levels of plasma lipoproteins. Such changes in the WD-fed *Ldlr*-KO rats were accompanied by hyperinsulinemia, obesity, and insulin resistance and — importantly with the formation of inflammatory atherosclerotic lesions — containing high levels of macrophages and cytokines. Thus, it appears that persistent hypercholesterolemia secondary to the deletion of *Ldlr* could promote systemic inflammation and multiple tissue dysfunction.

The hyperinsulinemia, insulin resistance, and obesity due to WD in *Ldlr*-KO rats is also observed in *Ldlr*-KO mice, but this diet also accelerates atherogenesis in these mice (53). Hence, it is difficult to estab-

lish whether the more severe insulin resistance in these mice is due to diet, dyslipidemia, or the formation of atherosclerotic lesions. Because atherosclerosis is an inflammatory disease, it is possible that increases in systemic inflammation could promote insulin resistance; however, this possibility could not be examined in mice, as both insulin resistance and atherosclerotic lesions develop simultaneously with dyslipidemia in *Ldlr*-KO mice. In contrast, the unique obesogenic phenotype of *Ldlr*-KO rats clearly suggests that a primary defect in LDL metabolism, even in the absence of high-fat diet or atherosclerosis, could be a sufficient cause of obesity and glucose intolerance. It is currently believed that dyslipidemia in humans with diabetes is secondary to insulin resistance that promotes lipid abnormalities, leading to a decrease in hepatic apoB degradation and increased secretion of triglyceride-rich VLDL particles. However, our observations suggest that the reverse is also possible. Defects in LDL metabolism that result in secondary changes in VLDL and triglycerides could lead to adipocyte hypertrophy, ectopic lipid deposition, and systemic glucose intolerance, suggesting that under some metabolic conditions dyslipidemia could be a cause rather than a consequence of obesity and glucose intolerance.

The obesogenic effects of *Ldlr* deletion observed in the rat are apparently different from those seen in humans. Not all patients with FH are frankly obese or insulin resistant, and even though hypertriglyceridemia is not considered to be a central feature of FH, most patients with homozygous FH have 2- to 3-fold increases in triglycerides (25), a phenotype similar to that observed in rats but not in mice. However, in patients of heterozygous FH, fasting triglycerides have been reported to be decreased by 10 % (54), and these patients are protected from type 2 diabetes as compared with their family members; hence, the phenotype in *Ldlr*-KO rats seems to be different from that in humans with heterozygous FH. However, in humans, familial combined hypercholesterolemia (FCH), in comparison with FH, is more closely associated with elevated blood glucose and insulin levels and adipocyte abnormalities (55, 56). FCH is the most prevalent genetic dyslipidemia in Western society (1:100) and is considered to be due to multiple defects that differ between families. It is associated with hepatic overproduction of VLDL particles, insulin resistance, hepatic fat accumulation, and impaired clearance of apoB-containing particles (56), defects similar to those seen in the *Ldlr*-KO rats. Moreover, like the *Ldlr*-KO rats, a substantial proportion of FCH patients have decreased LPL activity (57). Thus, the *Ldlr*-KO rat model could provide further insights into specific relationships between LDLR function and mixed hyperlipidemia.

The rat model could also be useful in disentangling the relationship between glucose intolerance and atherosclerotic lesion formation. Atherosclerotic lesions do not develop in *Ldlr*-KO mice fed a NC diet (6), and while feeding a WD leads to the formation of atherosclerotic lesions in these mice, they develop insulin resistance contemporaneously with atherosclerotic lesion formation (42, 43). Therefore, in these mice, it is difficult to untangle atherosclerotic changes from changes in glucose or lipid metabolism. There is a similar problem in studying atherogenesis and its relationship to obesity and insulin resistance in *apoe*-KO mice, which are resistant to diet-induced obesity and insulin resistance (44). In contrast, because the *Ldlr*-KO rats maintained on NC did not develop atherosclerotic lesions, it may be possible to study the effects of dyslipidemia on obesity and glucose homeostasis, independent of atherosclerotic lesions formation. Moreover, like atherogenesis in humans, atherosclerotic lesion formation in rats is slow and is preceded by glucose intolerance and obesity. *Ldlr*-KO mice, like the *Ldlr*-KO rats, do not develop atherosclerotic lesions on NC, but their cholesterol levels usually remain below 250 mg/dl (53). NC fed *Ldlr*-KO rats, in contrast, did not develop atherosclerotic lesions, even when their cholesterol levels exceeded 400 mg/dl. Atherosclerotic lesions in KO rats appeared only when cholesterol levels were consistently > 1,000 mg/dl for > 34 weeks. In comparison, *Ldlr*-KO (and *apoe*-KO) mice develop intermediate to advanced lesions within 10–20 weeks of WD (53, 58). Thus, it appears that more prolonged hypercholesterolemia is required to induce atherosclerotic lesion formation in rats than in mice, and because atherogenesis in these rats is slow and preceded by the obesity and insulin resistance, these rats might be more useful for studying the relationship between lipid and glucose metabolism and the contribution of metabolic changes to atherosclerotic lesion formation than either the *Ldlr*-KO or the *apoe*-KO mice. Furthermore, because in contrast to mice, rats are larger, they may be more amenable to surgical operations than mice, and they could provide larger biological samples (tissue, blood, urine), which would facilitate biochemical and histological measurements. In addition, in contrast to pigs and rabbits, rats have lower breeding costs and several rat models of metabolic disease have been developed that could be readily combined with the *Ldlr*-KO model.

Methods

Animal housing and diet. *Ldlr*-KO rats were generated at SAGE laboratory. Briefly, a total of 337 bp were deleted at the junction of intron 3 and exon 4 (on chromosome 8), and 4 bp ccgt were inserted using the zinc finger technology. The deletion was performed with the following sequence: agagacaggtgtgttgtagctttctgggcctttgcctactaccaccatgttttttgaggcacagggtcctgtctgtgagtaggctggtgtgtggtggtatgagccatagcatgacagggcgctctcctctctgtgcacccccacagcccccaagacgtgctccctggatgagttccgctgccaggatggcaagtgcatctcccggcagtttgtgtgtgaccaagactgggattgcctggatggctctgacgaggcccactgtgcggccaccacttgtggccctgctcacttccgctgcaactcctcttcctgcatccccagcctgtgggcctgcga. Details of the Zinc Finger Nuclease kits are described in Supplemental Tables 1–3. Zinc finger nucleases transcribed mRNA (in vitro) were injected in rat embryos at 5 ng/μl concentration. A total of 299 embryos were injected, out of which 181 embryos survived and transferred into 4 recipients. This resulted in the birth of 35 pups. One out of 35 pups was mutant. Although, the rate of indel generation was low in these rats, the resultant rat was fertile and sufficient to establish the colony of *Ldlr*-KO rats. Efficiency of indel generation may be improved by CRISPR/Cas9-targeted genome editing (59).

Experiments were performed in rats that were crossed for 5–7 generations on Sprague-Dawley background. Six-week-old male *Ldlr*-KO and WT Sprague-Dawley rats (Harlan laboratories) were housed under pathogen-free conditions in the University of Louisville vivarium under controlled temperature and 12-hour light/12-hour dark cycle and maintained on NC (5.5% fat; LabDiet). Starting at 12 weeks of age, rats were either fed WD (42% fat; Harlan Laboratories; WT [n = 10] and *Ldlr*-KO [n = 16]) or continued to be maintained on NC (WT [n = 9] and LDLR-KO [n = 8]). Rats were euthanized after 16, 34, 42, and 52 weeks of WD, and their plasma, heart, aorta and liver were harvested.

RNA isolation and quantitative PCR analyses. Primers for lipoprotein receptors were obtained from Qiagen, and quantitative PCR (qPCR) analysis was performed as described (60).

Western blot analyses. Anti-LDLR (AB30532; 1:1,000) and anti-ABCA1 (AB.H10; 1:1,000) antibodies were obtained from Abcam; anti-ABCG1 antibody (NB110-55438; 1:5,000) was purchased from Novus Biologicals; and anti-tublin antibody (T6074; 1:3,000) was bought from Sigma-Aldrich. Western blotting was performed on liver homogenates using standard techniques.

Blood glucose and plasma lipoprotein analyses. Blood was collected every 4 weeks from the tail vein after a 6-hour fast, and blood glucose was measured by an ACCU-CHEK Aviva glucometer. Levels of cholesterol and triglycerides in the plasma were measured as described (61, 62). For the quantitation of cholesterol and triglycerides in the liver, the tissue was pulverized and lipids were extracted as described by Bligh and Dyer (63). Solvents were evaporated under nitrogen, and the residue was dissolved in 5% BSA. Cholesterol and triglycerides were measured as described above. Cholesterol distribution in the lipoproteins was assessed by size-exclusion chromatography on FPLC (62). Particle size of lipoproteins was measured by NMR as described (64).

Hepatic triglyceride secretion. Hepatic triglyceride secretion rate was measured as described by Huang et al. (65). Briefly, rats were fasted overnight to remove the chylomicrons from the plasma. After obtaining the baseline samples, the rats received a bolus injection of tyloxapol (triton WR1339, Sigma-Aldrich; 300 mg/kg, i.v.) in the tail vein. Blood samples were collected at 0, 60, 90, 120, and 150 minutes after tyloxapol injection, and triglyceride content was measured in the plasma. Triglyceride secretion rates for each rat were calculated by simple linear regression plasma triglyceride levels (mg/kg body weight) as the dependent variable and time of measurement (hours) as the independent variable.

Glucose and insulin tolerance test. GTTs were performed after a 18-hour fast by injecting D-glucose (1 g/kg; i.p.) in sterile saline as described (66). Insulin tolerance tests were performed on nonfasted animals by injecting Humulin R (1.5 U/kg, i.p.; Lilly) (66).

Clinical chemistry parameters. Total protein, albumin, ALT, AST, creatinine, CK, and NEFA in the plasma were measured on MIRA chemical analyzer as described (64).

ELISAs. Levels of leptin (Eve Technologies Corporation), adiponectin (R&D Systems), insulin (Mercodia), PCSK9 (MBL International), fibrinogen (Innovative Research), PAI-1 (Innovative Research), apoB (MyBioSource), apolipoprotein A-V (Navatein Biosciences), and lipoprotein lipase (Antibody Research) in the plasma were measured by ELISA as per manufacturers' instructions. Plasma lipoprotein lipase activity was measured using the kit from Cell Biolabs Inc. (catalog STA-610).

Electrophoresis of apoB100 and apoB48. Plasma VLDL was isolated by ultracentrifugation (67). The VLDL was delipidated, electrophoresed on a 3% acrylamide gel (in house), and silver stained (24).

Atherosclerotic lesion analysis. Lesions were examined throughout the aortic tree as described (61, 62, 64, 68). Lesions in the aortic valve were examined in the OCT-fixed sections at 2× magnification following

staining with Oil Red O. Lesions in the enfaced aorta were visualized with Sudan IV staining. Lesions in the coronary artery were examined after staining with H&E.

Immunohistochemical analysis. Immunohistochemical analyses was performed on formalin-fixed sections of abdominal aortae as described before (62, 68). Briefly, sections (5 μm) were deparaffinized and rehydrated. Sections were incubated with anti-CD68 (MCA1957A647, clone FA-11, Bio-Rad), anti-TNFα, anti–MCP-1, and anti–IL-6 (ab6671, ab25124, and ab9324, respectively; Abcam) antibodies for 18 hours at 4°C followed by staining with and goat anti–rabbit or anti–mouse IgG – Alx488 (A11008 and A11001, respectively, Invitrogen). Digital images were acquired at ×60 magnification.

Statistics. Data are expressed as mean ± SEM. Unpaired 2-tailed Student's *t* test was used for the data analysis when the data were restricted to 2 groups. Two-way ANOVA followed by Bonferroni post-tests were used to compare more than 2 experimental groups. Statistical significance was accepted at $P < 0.05$ level.

Study approval. Animal protocols for the study were approved by University of Louisville animal care and use committee (IACUC number 16670).

Author contributions

SS and AB designed the experiments, did the critical analyses of data, provided the resources, and wrote the manuscript. SDS, MVM, NSW, AA, AK, and REHB performed the experiments, acquired and analyzed the data, and wrote sections of the manuscripts. KAR, MGW, and DWR performed the experiments, acquired data, and performed data analyses.

Acknowledgments

This work was supported in parts by NIH grants HL95593, HL120746, and ES17260 (to SS) and GM 103492, and P50 HL120163 to (AB).

Address correspondence to: Sanjay Srivastava, Department of Medicine, Division of Cardiovascular Medicine, 204 F, Delia Baxter Building, 580 South Preston Street, University of Louisville, Louisville, Kentucky 40202, USA. Phone: 502.852.5834; E-mail: sanjay@louisville.edu.

1. Nicholls SJ, et al. Effect of two intensive statin regimens on progression of coronary disease. *N Engl J Med*. 2011;365(22):2078–2087.
2. Getz GS, Reardon CA. Animal models of atherosclerosis. *Arterioscler Thromb Vasc Biol*. 2012;32(5):1104–1115.
3. Bang C, et al. Cardiac fibroblast-derived microRNA passenger strand-enriched exosomes mediate cardiomyocyte hypertrophy. *J Clin Invest*. 2014;124(5):2136–2146.
4. Weber C, Noels H. Atherosclerosis: current pathogenesis and therapeutic options. *Nat Med*. 2011;17(11):1410–1422.
5. Buja LM, Kita T, Goldstein JL, Watanabe Y, Brown MS. Cellular pathology of progressive atherosclerosis in the WHHL rabbit. An animal model of familial hypercholesterolemia. *Arteriosclerosis*. 1983;3(1):87–101.
6. Ishibashi S, Goldstein JL, Brown MS, Herz J, Burns DK. Massive xanthomatosis and atherosclerosis in cholesterol-fed low density lipoprotein receptor-negative mice. *J Clin Invest*. 1994;93(5):1885–1893.
7. Zhang SH, Reddick RL, Piedrahita JA, Maeda N. Spontaneous hypercholesterolemia and arterial lesions in mice lacking apolipoprotein E. *Science*. 1992;258(5081):468–471.
8. Plump AS, et al. Severe hypercholesterolemia and atherosclerosis in apolipoprotein E-deficient mice created by homologous recombination in ES cells. *Cell*. 1992;71(2):343–353.
9. Maeda N. Development of apolipoprotein E-deficient mice. *Arterioscler Thromb Vasc Biol*. 2011;31(9):1957–1962.
10. Tavori H, et al. Serum proprotein convertase subtilisin/kexin type 9 and cell surface low-density lipoprotein receptor: evidence for a reciprocal regulation. *Circulation*. 2013;127(24):2403–2413.
11. Brown MS, Goldstein JL. Lipoprotein receptors in the liver. Control signals for plasma cholesterol traffic. *J Clin Invest*. 1983;72(3):743–747.
12. Davidson NO, Powell LM, Wallis SC, Scott J. Thyroid hormone modulates the introduction of a stop codon in rat liver apolipoprotein B messenger RNA. *J Biol Chem*. 1988;263(27):13482–13485.
13. Sharma V, Forte TM, Ryan RO. Influence of apolipoprotein A-V on the metabolic fate of triacylglycerol. *Curr Opin Lipidol*. 2013;24(2):153–159.
14. Ason B, et al. PCSK9 inhibition fails to alter hepatic LDLR, circulating cholesterol, and atherosclerosis in the absence of ApoE. *J Lipid Res*. 2014;55(11):2370–2379.
15. Brown MS, Goldstein JL. A receptor-mediated pathway for cholesterol homeostasis. *Science*. 1986;232(4746):34–47.
16. Jeon H, Blacklow SC. Structure and physiologic function of the low-density lipoprotein receptor. *Annu Rev Biochem*. 2005;74:535–562.
17. Watanabe Y. Serial inbreeding of rabbits with hereditary hyperlipidemia (WHHL-rabbit). *Atherosclerosis*. 1980;36(2):261–268.
18. Herrera VL, et al. Spontaneous combined hyperlipidemia, coronary heart disease and decreased survival in Dahl salt-sensitive hypertensive rats transgenic for human cholesteryl ester transfer protein. *Nat Med*. 1999;5(12):1383–1389.
19. Prescott MF, McBride CH, Hasler-Rapacz J, Von Linden J, Rapacz J. Development of complex atherosclerotic lesions in pigs

with inherited hyper-LDL cholesterolemia bearing mutant alleles for apolipoprotein B. *Am J Pathol*. 1991;139(1):139–147.
20. Davis BT, et al. Targeted disruption of LDLR causes hypercholesterolemia and atherosclerosis in Yucatan miniature pigs. *PLoS One*. 2014;9(4):e93457.
21. Al-Mashhadi RH, et al. Familial hypercholesterolemia and atherosclerosis in cloned minipigs created by DNA transposition of a human PCSK9 gain-of-function mutant. *Sci Transl Med*. 2013;5(166):166ra1.
22. Asahina M, et al. Hypercholesterolemia and atherosclerosis in low density lipoprotein receptor mutant rats. *Biochem Biophys Res Commun*. 2012;418(3):553–558.
23. Scott J. The molecular and cell biology of apolipoprotein-B. *Mol Biol Med*. 1989;6(1):65–80.
24. Windmueller HG, Spaeth AE. Regulated biosynthesis and divergent metabolism of three forms of hepatic apolipoprotein B in the rat. *J Lipid Res*. 1985;26(1):70–81.
25. James RW, et al. Apolipoprotein B metabolism in homozygous familial hypercholesterolemia. *J Lipid Res*. 1989;30(2):159–169.
26. Twisk J, Gillian-Daniel DI, Tebon A, Wang L, Barrett PH, Attie AD. The role of the LDL receptor in apolipoprotein B secretion. *J Clin Invest*. 2000;105(4):521–532.
27. Huang Y, et al. Overexpression and accumulation of apolipoprotein E as a cause of hypertriglyceridemia. *J Biol Chem*. 1998;273(41):26388–26393.
28. Lambert G, et al. Fasting induces hyperlipidemia in mice overexpressing proprotein convertase subtilisin kexin type 9: lack of modulation of very-low-density lipoprotein hepatic output by the low-density lipoprotein receptor. *Endocrinology*. 2006;147(10):4985–4995.
29. Herbert B, et al. Increased secretion of lipoproteins in transgenic mice expressing human D374Y PCSK9 under physiological genetic control. *Arterioscler Thromb Vasc Biol*. 2010;30(7):1333–1339.
30. Wilson DE, et al. Phenotypic expression of heterozygous lipoprotein lipase deficiency in the extended pedigree of a proband homozygous for a missense mutation. *J Clin Invest*. 1990;86(3):735–750.
31. Schaap FG, et al. ApoAV reduces plasma triglycerides by inhibiting very low density lipoprotein-triglyceride (VLDL-TG) production and stimulating lipoprotein lipase-mediated VLDL-TG hydrolysis. *J Biol Chem*. 2004;279(27):27941–27947.
32. Grosskopf I, et al. Apolipoprotein A-V deficiency results in marked hypertriglyceridemia attributable to decreased lipolysis of triglyceride-rich lipoproteins and removal of their remnants. *Arterioscler Thromb Vasc Biol*. 2005;25(12):2573–2579.
33. Merkel M, et al. Apolipoprotein AV accelerates plasma hydrolysis of triglyceride-rich lipoproteins by interaction with proteoglycan-bound lipoprotein lipase. *J Biol Chem*. 2005;280(22):21553–21560.
34. Marçais C, et al. Apoa5 Q139X truncation predisposes to late-onset hyperchylomicronemia due to lipoprotein lipase impairment. *J Clin Invest*. 2005;115(10):2862–2869.
35. Kersten S. Physiological regulation of lipoprotein lipase. *Biochim Biophys Acta*. 2014;1841(7):919–933.
36. Do R, et al. Exome sequencing identifies rare LDLR and APOA5 alleles conferring risk for myocardial infarction. *Nature*. 2015;518(7537):102–106.
37. Nilsson SK, Heeren J, Olivecrona G, Merkel M. Apolipoprotein A-V; a potent triglyceride reducer. *Atherosclerosis*. 2011;219(1):15–21.
38. Matsubara M, Maruoka S, Katayose S. Decreased plasma adiponectin concentrations in women with dyslipidemia. *J Clin Endocrinol Metab*. 2002;87(6):2764–2769.
39. Hotta K, et al. Plasma concentrations of a novel, adipose-specific protein, adiponectin, in type 2 diabetic patients. *Arterioscler Thromb Vasc Biol*. 2000;20(6):1595–1599.
40. Qiao L, Zou C, van der Westhuyzen DR, Shao J. Adiponectin reduces plasma triglyceride by increasing VLDL triglyceride catabolism. *Diabetes*. 2008;57(7):1824–1833.
41. Grundy SM. Atherosclerosis imaging and the future of lipid management. *Circulation*. 2004;110(23):3509–3511.
42. Ngai YF, et al. Ldlr-/- mice display decreased susceptibility to Western-type diet-induced obesity due to increased thermogenesis. *Endocrinology*. 2010;151(11):5226–5236.
43. Schreyer SA, Vick C, Lystig TC, Mystkowski P, LeBoeuf RC. LDL receptor but not apolipoprotein E deficiency increases diet-induced obesity and diabetes in mice. *Am J Physiol Endocrinol Metab*. 2002;282(1):E207–E214.
44. Karagiannides I, Abdou R, Tzortzopoulou A, Voshol PJ, Kypreos KE. Apolipoprotein E predisposes to obesity and related metabolic dysfunctions in mice. *FEBS J*. 2008;275(19):4796–4809.
45. Demers A, et al. PCSK9 Induces CD36 Degradation and Affects Long-Chain Fatty Acid Uptake and Triglyceride Metabolism in Adipocytes and in Mouse Liver. *Arterioscler Thromb Vasc Biol*. 2015;35(12):2517–2525.
46. Seidah NG, Awan Z, Chrétien M, Mbikay M. PCSK9: a key modulator of cardiovascular health. *Circ Res*. 2014;114(6):1022–1036.
47. Mbikay M, et al. PCSK9-deficient mice exhibit impaired glucose tolerance and pancreatic islet abnormalities. *FEBS Lett*. 2010;584(4):701–706.
48. Miyamoto Y, Shimada K, Sakaguchi Y, Miyamoto M. Cisplatin (CDDP)-induced acute toxicity in an experimental model of hepatic fibrosis. *J Toxicol Sci*. 2007;32(3):311–319.
49. Arya A, Yadav HN, Sharma PL. Involvement of vascular endothelial nitric oxide synthase in development of experimental diabetic nephropathy in rats. *Mol Cell Biochem*. 2011;354(1-2):57–66.
50. Huang Q, et al. AIP1 suppresses atherosclerosis by limiting hyperlipidemia-induced inflammation and vascular endothelial dysfunction. *Arterioscler Thromb Vasc Biol*. 2013;33(4):795–804.
51. Yaluri N, et al. Simvastatin Impairs Insulin Secretion by Multiple Mechanisms in MIN6 Cells. *PLoS ONE*. 2015;10(11):e0142902.
52. Zhao SP, Wu J. Fenofibrate reduces tumor necrosis factor-alpha serum concentration and adipocyte secretion of hypercholesterolemic rabbits. *Clin Chim Acta*. 2004;347(1-2):145–150.
53. Merat S, Casanada F, Sutphin M, Palinski W, Reaven PD. Western-type diets induce insulin resistance and hyperinsulinemia in LDL receptor-deficient mice but do not increase aortic atherosclerosis compared with normoinsulinemic mice in which similar plasma cholesterol levels are achieved by a fructose-rich diet. *Arterioscler Thromb Vasc Biol*. 1999;19(5):1223–1230.
54. Besseling J, Kastelein JJ, Defesche JC, Hutten BA, Hovingh GK. Association between familial hypercholesterolemia and prevalence of type 2 diabetes mellitus. *JAMA*. 2015;313(10):1029–1036.

55. van der Vleuten GM, et al. Elevated leptin levels in subjects with familial combined hyperlipidemia are associated with the increased risk for CVD. *Atherosclerosis*. 2005;183(2):355–360.
56. Brouwers MC, van Greevenbroek MM, Stehouwer CD, de Graaf J, Stalenhoef AF. The genetics of familial combined hyperlipidaemia. *Nat Rev Endocrinol*. 2012;8(6):352–362.
57. Babirak SP, Brown BG, Brunzell JD. Familial combined hyperlipidemia and abnormal lipoprotein lipase. *Arterioscler Thromb*. 1992;12(10):1176–1183.
58. Nakashima Y, Plump AS, Raines EW, Breslow JL, Ross R. ApoE-deficient mice develop lesions of all phases of atherosclerosis throughout the arterial tree. *Arterioscler Thromb*. 1994;14(1):133–140.
59. Gupta RM, Musunuru K. Expanding the genetic editing tool kit: ZFNs, TALENs, and CRISPR-Cas9. *J Clin Invest*. 2014;124(10):4154–4161.
60. Vladykovskaya E, et al. Lipid peroxidation product 4-hydroxy-trans-2-nonenal causes endothelial activation by inducing endoplasmic reticulum stress. *J Biol Chem*. 2012;287(14):11398–11409.
61. Barski OA, et al. Dietary carnosine prevents early atherosclerotic lesion formation in apolipoprotein E-null mice. *Arterioscler Thromb Vasc Biol*. 2013;33(6):1162–1170.
62. Srivastava S, et al. Aldose reductase protects against early atherosclerotic lesion formation in apolipoprotein E-null mice. *Circ Res*. 2009;105(8):793–802.
63. Bligh EG, Dyer WJ. A rapid method of total lipid extraction and purification. *Can J Biochem Physiol*. 1959;37(8):911–917.
64. Srivastava S, et al. Oral exposure to acrolein exacerbates atherosclerosis in apoE-null mice. *Atherosclerosis*. 2011;215(2):301–308.
65. Huang W, Dedousis N, Bandi A, Lopaschuk GD, O'Doherty RM. Liver triglyceride secretion and lipid oxidative metabolism are rapidly altered by leptin in vivo. *Endocrinology*. 2006;147(3):1480–1487.
66. Sansbury BE, et al. Overexpression of endothelial nitric oxide synthase prevents diet-induced obesity and regulates adipocyte phenotype. *Circ Res*. 2012;111(9):1176–1189.
67. Chung BH, et al. Single vertical spin density gradient ultracentrifugation. *Meth Enzymol*. 1986;128:181–209.
68. Baba SP, et al. Reductive metabolism of AGE precursors: a metabolic route for preventing AGE accumulation in cardiovascular tissue. *Diabetes*. 2009;58(11):2486–2497.